



HAL
open science

Fire gilding investigation on early medieval copper-based jewellery by focused ion beam (FIB) on FEG-SEM

Estelle Ottenwelter, Claudie Josse, Arnaud Proietti, Luc Robbiola

► To cite this version:

Estelle Ottenwelter, Claudie Josse, Arnaud Proietti, Luc Robbiola. Fire gilding investigation on early medieval copper-based jewellery by focused ion beam (FIB) on FEG-SEM. *Journal of Archaeological Science: Reports*, 2022, 46, pp.103602. 10.1016/j.jasrep.2022.103602 . hal-04210011

HAL Id: hal-04210011

<https://hal.science/hal-04210011v1>

Submitted on 18 Sep 2023

HAL is a multi-disciplinary open access archive for the deposit and dissemination of scientific research documents, whether they are published or not. The documents may come from teaching and research institutions in France or abroad, or from public or private research centers.

L'archive ouverte pluridisciplinaire **HAL**, est destinée au dépôt et à la diffusion de documents scientifiques de niveau recherche, publiés ou non, émanant des établissements d'enseignement et de recherche français ou étrangers, des laboratoires publics ou privés.

Fire gilding investigation on early medieval copper-based jewellery by focused ion beam (FIB) on FEG-SEM

Estelle Ottenwelter^{a,b,*}, Claudie Josse^c, Arnaud Proietti^c, Luc Robbiola^b

^a *Institute of Archaeology CAS Prague, v.v.i., Letenska 4, 118 01 Praha 1, Czech Republic*

^b *TRACES Laboratory (CNRS UMR5608), Université de Toulouse, Maison de la Recherche, 31058 Toulouse Cedex 9, France*

^c *Centre de Microcaractérisation Raimond Castaing (CNRS UAR 3623), Espace Clement Ader, 3 rue Caroline Aigle, 31400 Toulouse, France*

ABSTRACT

The study of ancient gilding is often problematic, as the gilding layers are soft and prone to deformation during sample preparation. In this respect, focused ion beam (FIB) milling on a field emission gun scanning electron microscope (FEG-SEM) provides poorly invasive *in situ* sampling. The operating process is here detailed and applied on gilded medieval copper-based elite jewellery (10th century) from Prague Castle. Obtained cross-sections and slices of gilded samples were investigated up to nanometer scale without gilding layer deformation. By coupling structural observation with elemental X-ray analysis (EDS) and electron beam diffraction (EBSD), FIB FEG-SEM provided new data on the physical-chemical characteristics of the gilded layer. The gilding has a two-layer metallurgical structure containing a quaternary Au (Hg, Cu, Ag) alloy corresponding to the gold solid solution fcc phase, and a submicrometric inner sublayer formed by a Au-Cu phase, relative to the inter-diffusion of copper from the substrate during the fire gilding process. The applied temperature for gilding can be estimated at c. 400 °C. Sintering of the mercury-gold amalgam globules during the fire heating is highlighted. The precise characterisation of the gilding layers provided useful comparative parameters for identifying fire gilding skill levels and assessing the overall quality of the archaeological pieces.

Keywords: Fire gilding, Jewellery, FIB milling, Middle ages, Central Europe Interdiffusion, Electron channeling contrast.

1. Introduction

This work characterises the gilding of ancient medieval jewellery by applying the new method of a focused ion beam (FIB) mounted on a field emission gun – scanning electron microscope (FEG-SEM). The study focuses on central European gilded copper jewellery, for which fire gilding was largely applied (Ottenwelter, *in press*). It concerns the fire gilding layers of specific archaeological artefacts found in Bohemia (Lumbe Garden cemetery at Prague Castle): *gombiky* (spherical hollow pendants) and medallions, characteristic pieces of the elite jewellery from the 9th and 10th centuries AD, detailed in previous studies (Ottenwelter et al., 2014; Ottenwelter et al., 2017; Ottenwelter et al., 2020; Ottenwelter, *in press*). The use of FIB FEG-SEM allows cross-sections to be made and observations performed *in situ* within the SEM (Johnson et al., 2012; Chiavari et al., 2015; Masi et al., 2016; Masi et al., 2017). As discussed in the experimental part, FIB allows very accurate *in situ* sampling without damage to multi-layer materials compared to conventional mechanical means (Goldstein et al., 2003, 557). This new

approach is thus particularly interesting for the study of cultural heri-tage artefacts, which are often fragile, fragmented or corroded.

Gilding is a decorative technique commonly applied since antiquity in the Mediterranean world (Oddy, 1993, 2000), in the Near East (Gunter and Jett, 1992) as well as in Asia (Jett and Chase, 2000; Mur-akami, 2000; Shin et al., 2020). In Europe, it was widespread in the Middle Ages (Dandridge, 2000; Masi et al., 2016; Ottenwelter, *in press*). The thin gold layer applied to less valuable material (metal, wood, bone) gives the appearance of solid gold (Oddy, 1993, 171). This technique was used, e.g., on sculptures, bas-reliefs, and roofs, and was also commonly used on jewellery.

In 9th- and 10th-century central Europe, gilding was widely used in the manufacture of elite jewellery and dress accessories. The most common gilding method during this period was **fire gilding**, also referred to as **mercury gilding or amalgam gilding**, which involved preparing a gold amalgam with mercury. Mercury gilding is traditionally obtained by mixing gold (in the form of solid leaves or filings) with mercury (liquid) to create a paste with an overall composition of 80–90

* Corresponding author at: Institute of Archaeology CAS Prague, v.v.i., Letenska 4, 118 01 Praha 1, Czech Republic.

E-mail addresses: ottenwelter@arup.cas.cz (E. Ottenwelter), claudie.josse@ums-castaing.fr (C. Josse), arnaud.proietti@ums-castaing.fr (A. Proietti), robbiola@univ-tlse2.fr (L. Robbiola).

wt% Hg and 10–20 wt% Au (Anheuser 1997). This gilding paste is spread over the copper surface, previously cleaned using a corrosive agent (such as a solution of alum and rock salt in acetic acid) to remove the thin copper oxide layer formed in the atmosphere (Anheuser 1997, 58–59; Northover and Anheuser 2000, 116). The copper artefact was heated for a few minutes to 250°C — 350°C until the surface turned from grey to dull yellow as the mercury volatilised (Northover and Anheuser 2000, 118). The resulting gilded surface, lighter due to the significant evaporation of mercury, is porous and still contains residual mercury. It is then burnished with a hard and polished stone to close the porous structure and give a smooth and reflective surface, often creating parallel striations on the surface. Unburnished surfaces are highly porous and are often still visible in recesses.

In contrast to the gilding of a plain cast artefact, the gilding of Moravian and Bohemian elite jewels during the early medieval period required great skill. It was used on composite artefacts soldered and decorated mostly by chasing or granulation (Ottenwelter et al., 2014; Ottenwelter et al., 2017; Ottenwelter, in press). Great skill in gilding was thus required to avoid flooding the decoration.

The different types of elite jewellery and their evolution in construction, decorative techniques, materials and motifs observed between various regions are important chronological markers. Among these markers, the gilding technology and its quality offers additional keys for differentiating fine products produced by highly skilled jewellers operating in the courtly environment and coarse imitations produced by local and less experienced craftsmen.

In this respect, the identification of the gilding technique based on a detailed study of the gilding layer is crucial for determining the level of skill achieved by ancient jewellers, for pointing out different know-how or workshops and for distinguishing local from imported products. This requires a precise characterisation of the gilding layer. As pure or low-alloyed noble metals (copper, silver and gold) are soft metals, conventional means of investigation at different scales (Sandu et al., 2011), including metallography, often deform the surface during sample preparation steps, causing inaccurate measurements, especially on the thickness and compactness of the gilding, and negatively affecting the accuracy of the metallographic investigation.

In this study, three fragments of Bohemian gilded copper ornaments — two hollow spherical pendants known as *gombiky* (Tab. 1.1, Tab. 1.2) and one medallion (Tab. 1.3) — dated to the first half of the 10th century CE, were investigated using FIB FEG-SEM to obtain new data on the structure and composition of the gilded layer and to evaluate the fire gilding skill level of the ancient craftsmen.

2. Archaeological context




All the investigated pieces of jewellery (Table 1) were recovered from the Lumbe Garden cemetery at Prague Castle, where the ruling elite and their retinue were buried from the second half of the 9th until the 11th century (Frolík and Smetánka 2014). After the fall of Great Moravia in the early 10th century, Prague Castle became a major political, ecclesiastical and economic centre in central Europe and the seat of the Bohemian rulers. The Lumbe Garden cemetery, one of the richest in Bohemia (Frolík 2014), was excavated in 1972–1976 by the Institute of Archaeology of Prague under the supervision of Z. Smetánka. The two investigated gilded fragments of copper *gombiky* (H84-1 and H115-9) were found in two particularly rich graves belonging to two females aged 10 and 14 (Table 1). As is often observed in funeral contexts, each of these investigated *gombiky* formed an identical pair with another *gombik* (H84-2 and H115-8) not studied here. The studied gilded fragment of the medallion (H52-2) was found in a more modest grave of a two-year-old child which contained a pair of gilded medallions, a knife and a ceramic pot (Frolík and Smetánka 2014, 105–106).

In this context, the two selected *gombiky* are well representative of Bohemian elite jewellery from the 10th century.

Medallions are also elite jewellery but are quite rare in Bohemia in

Table 1:

Investigated finds and their archaeological context (illustration after Frolík-Smetánka, 2014).

Object	Number	Illustration	Archaeological context
1. <i>Gombik</i>	H84-1		Grave No. 84, Prague Castle, Lumbe Garden: child, female, age 10, grave goods: 2 gilded copper <i>gombiky</i> , 5 silver grape-shaped earrings, 2 silver S-shaped temple rings, a copper alloy ring, 1 iron knife, a necklace with 25 amber and glass beads, eggshell.
2. <i>Gombik</i>	H115-8		Grave No. 115, Prague Castle, Lumbe Garden: female, age 14, grave goods: 2 gilded copper <i>gombiky</i> , 2 silver <i>gombiky</i> , 12 silver grape-shaped earrings, two iron knives.
3. Medallion	H52-2		Grave No. 52, Prague Castle, Lumbe Garden: child, age 2, grave goods: pair of gilded copper medallions, iron knife, gilded temple ring with an eyelet, ceramic pot.

this period and are most often considered imports. Other medallions found in Bohemia usually contained a cabochon or a cameo, such as the medallion found in Želenky, which was decorated with an antique cameo (Benda, 2002, plate 63), or the pair of silver medallions from Klecany II decorated with lead cabochons (Profantová, 2010, plate 95; Profantová, 2013, 35). The pair of gilded medallions from Lumbe Garden are now blank but were probably decorated with a cabochon or a cameo as well.

3. Material and methods

3.1. Materials – Gilded fragments

The three investigated fragments are gilded samples from representative gilded copper pieces of jewellery as previously reported in (Table 1) and shown in Figs. 1, 2 and 3. Here, the studied fragments are from artefacts of different technical qualities as detailed below. The gilding was in all cases applied after the assemblage and soldering of the various components, masking the construction and hard solders.

(i) The fragment of *gombik* H84-1 is a sample from a large *gombik* (total length: 55.6 mm, diameter: 44 mm - Fig. 1a) its construction is typical of Bohemian pieces, as shown from X-ray radiography (Fig. 1e): a two-hemisphere body and a suspension system made of three components (Ottenwelter et al., 2014; Ottenwelter et al., 2017; Ottenwelter et al., 2020): a loop, a clamp and a ring, in this case also including a small pellet inside the soldered hemispheres. The *gombik* was highly fragmented when excavated. It was re-restored in 2013 and the fragments assembled, but it remains incomplete and is in an advanced state of mineralisation.

The fragment is from one of the chased hemispheres, which could not be localised with certainty. It is about 3 mm wide and 0.2 mm thick, which corresponds to the hemisphere thickness. As illustrated in Fig. 1b–c, the gilded surface is covered by a coarse layer of corrosion species, bright red in colour and mainly related to cuprous oxide Cu₂O according to EDS surface analysis. The *gombik* was cleaned in the past by immersion in a chemical solution, which led to its fragmentation, as it is almost completely mineralised. Decohesion of the gilding from the copper

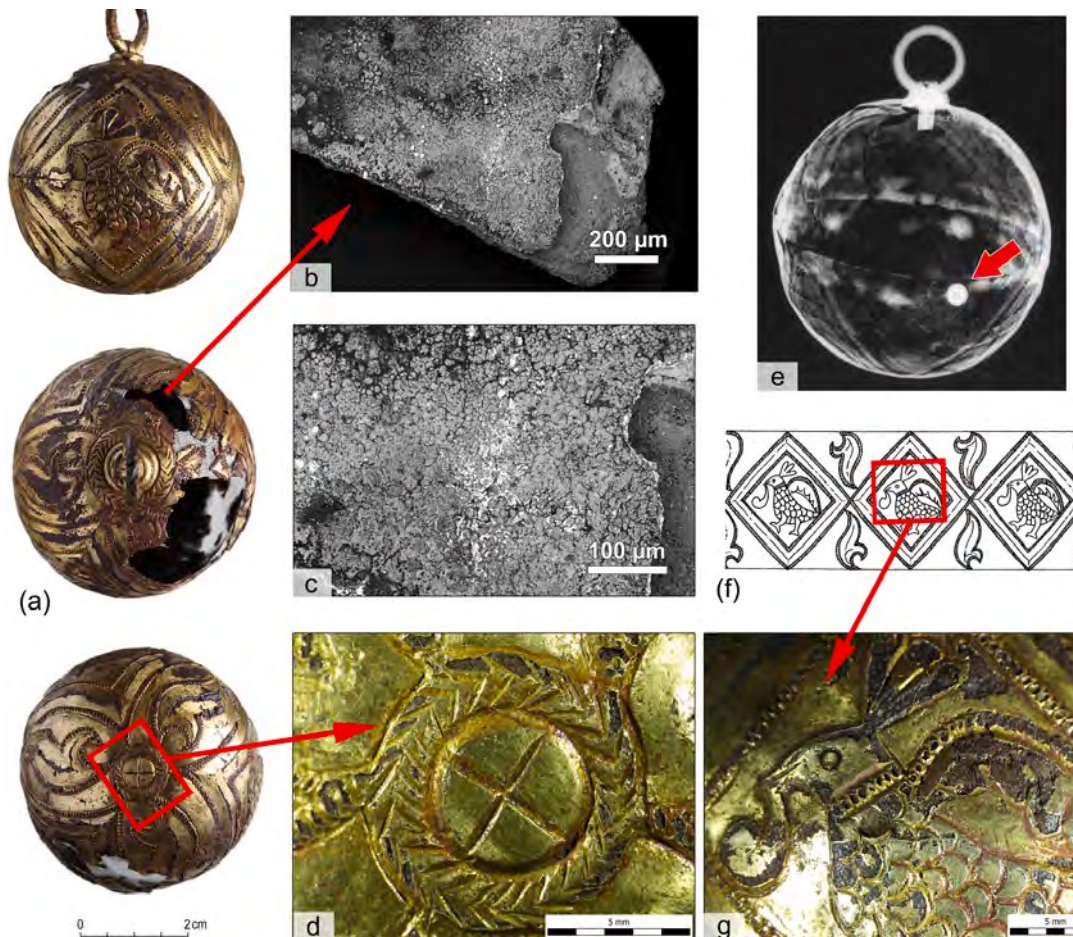


Fig. 1. Gombik H84-1: a - general view, profile, upper and lower poles; b–c - detail of the studied fragment and gilded surface, SEM micrograph (BSE); d - detail of the chased cross on the lower pole; e - X-ray radiograph revealing the mounting of the *gombik*; f - drawing of the chased decoration (Frolík-Smet'anka, 2014, 152); g - detail of the chased peacock.

substrate is observed in places, as seen on the edge of the studied fragment (Fig. 1c). This must be related to the corrosion of the substrate but could also be linked to the gilding quality. The overall quality of this jewellery is average. As regards the chasing, no preliminary sketch was made, no drawing compass was used and the chased decoration is slightly irregular. A cross in a circle decorated with chevrons is depicted at the lower pole (Fig. 1d). The circular surface is divided into three diamond panels, in the middle of which a peacock is represented holding a drop-shaped element in his beak and wearing a necklace (Fig. 1f–g). An inverse foliate ornament fills the spaces between the panels (Fig. 1f).

(ii) The fragment of *gombik* H115-9 is shown on Fig. 2; due to its very poor condition, its twin pair H115-8, in better condition, is used in Fig. 2 to illustrate the shape, mounting and drawing of this piece. The fragment is issued from a medium-sized *gombik* (full length: 40 mm, diameter: 30 mm). As for the previous *gombik* H84-1, the construction follows the same type and is also decorated with chasing (Fig. 2a). The gilded fragment of H115-9 (Fig. 2b–c) comes from a hemisphere. It is of about 4 mm wide and 0.2 mm thick, and bears part of the chased decoration of interlaced braids (Fig. 2d). The quality of the piece is high, as the chased decoration is very precise and regular. Depression marks (red arrow in Fig. 2f) reveal that a drawing compass was used to regularly place the motifs on the body of the object (Fig. 2a), with the interlacing braids forming three panels (Fig. 2d–e). In each panel, a medallion ornamented by chevrons is represented, in the middle of which is an 8-fold rosette (Fig. 2e–f) surrounded by arms (Manus Dei representation Fig. 2e).

(iii) The third studied fragment is related to another type of

jewellery: a gilded copper **medallion H52-2** (Fig. 3). The overall quality of the medallion is very high. It consists of five different parts joined together: a circular sheet 28.5 mm in diameter and 0.4 mm thick with two appendices of rectangular section forming circular rings, a loop, a rivet securing the loop to the rings and a chased sheet 0.2 mm thick forming the bezel (Fig. 3a). The bezel is decorated with a central chevron motif between two beaded rows (Fig. 3a, e). The circular sheet is perforated (Fig. 3a), perhaps to prevent the bursting of the object during soldering. The system of suspension is complex (Fig. 3d) and indicates high craftsmanship. However, the current condition of the medallion is rather poor – incomplete, brittle and in an advanced state of mineralisation. The surface of the gilding layer is tarnished and pitted (Fig. 3d, f). The studied fragment shown in Fig. 3b is around 5 mm wide and 2 mm thick. It corresponds to a small piece of the bezel, as shown in Fig. 3e on a large, well-preserved part. The cleaned surface fragment exhibits unburnished gilded areas in the recesses of the chased chevron, characterised by a high porosity and revealing gold micrometric globules (Fig. 3c).

3.2. Methods – FIB on FEG-SEM

To avoid damaging the gilding, FIB FEG-SEM was performed directly on the gilded medieval fragments. The apparatus used was a FEI Helios NanoLab 600i coupled with the Aztec Oxford EDS system (SDD detector, WD 4 mm), i.e., a dual-beam microscope combining a field emission electron gun (FEG) and a gallium ion column capable of delivering up to 65nA of current for surface milling. It is equipped with an EDS-3D

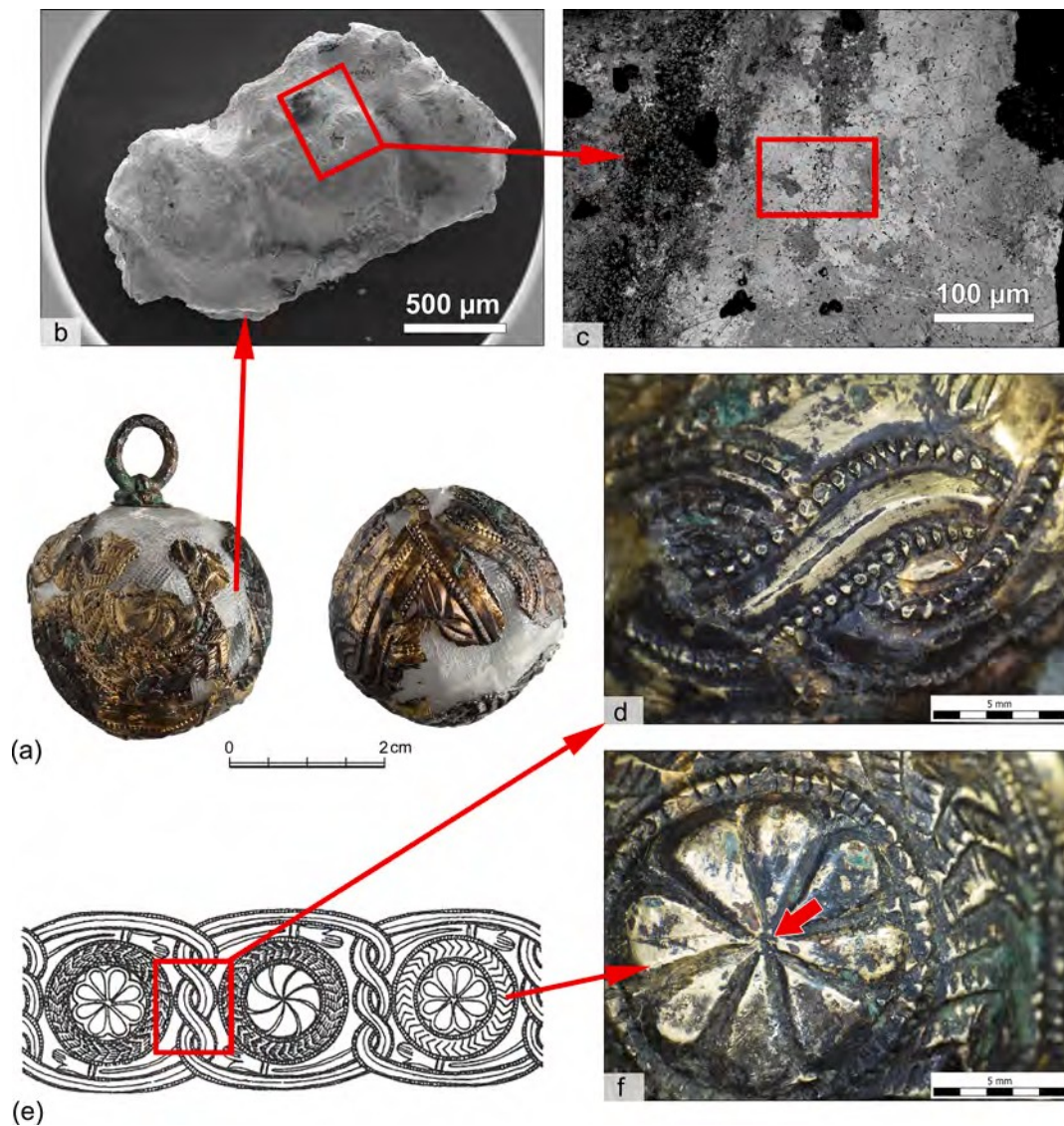


Fig. 2. Gombik H115-8 and 9: a - general view – profile and lower pole (*gombik* H115-8, twin artefact of H115-9); b-c - detail of the studied fragment (H115-9) and of the gilded surface, SEM micrographs (SE and BSE); d - detail of the chased interlaces (H115-8); e - drawing of the chased decoration (H115-8) (Frolík-Smet'anka, 2014, 188); f - detail of the eightfold chased rosette ornament (H115-8).

spectrometer for analysing composition and mapping chemical elements. An electron backscattered diffraction (EBSD) analysis was also performed on the H-84 sample using a CMOS EBSD camera (Symmetry S2, Oxford Instruments) mounted on an FEG-SEM JEOL JSM 7100F. EBSD mapping was performed at 20 kV accelerating voltage, with a step size of 50 nm and provided complementary morphological and crystallographic information on the gilded sublayers. On each gilded fragment, prior to SEM or EBSD investigation, a thin amorphous conductive layer of carbon (5–10 nm thick) was applied.

FIB FEG-SEM uses a beam of positively charged ions (Goldstein et al., 2003, 553) for milling a selected surface, thus obtaining a local cross-section 10–100 µm in width and about 10–30 µm in depth. In the present configuration, milling can be performed on fragments not exceeding 30 mm in size and 5 mm thick.

Two main powerful FIB approaches are used for sample preparation, both of which are very well suited to complex and fragile samples such as archaeological materials.

(i) The simplest approach is relative to the direct milling and *in situ* observation of a cross-section (Goldstein et al., 2003, 553–554). The different steps are shown in Fig. 4. After placement in the SEM chamber, the area of interest is selected from the general untilted view of the

sample and the section to be performed is then precisely determined (Fig. 4a). A thin layer of platinum (around 200 nm thick) is then applied on this section by electron beam (Fig. 4b). The deposition of a protective layer is always suggested for several reasons: to prevent the top surface of the sample from being damaged during subsequent ion milling and to minimise cross-section surface curtaining.

A preliminary regular cross-section pattern is defined so that it overlaps with the bottom edge of the Pt strip. An ionic ablation generated by Ga⁺ ions of a few nA (65nA) is applied to the surface sample to create a cross-section (Fig. 4c-d) as large as 100 µm in width and 10–20 µm in depth. As shown in Fig. 4e, at 0° tilt, the invasive intervention is equivalent to a quadrangular excavation of 100 × 50 µm² and about 30 µm deep, which is a very small volume hardly visible to the naked eye and therefore particularly suitable for cultural materials. A final milling operating at a lower ion current is performed for obtaining a very accurate final thin “polishing” at a nanometric resolution. As shown on the sample at 52° tilt (Fig. 4f), detailed structural information can be observed, documented and analysed. An elemental X-ray profile and mapping can thus be performed on different areas of the cross-section revealing phenomena such as the porosity of the gilding layer, the residual level of mercury or the interdiffusion of metallic elements from

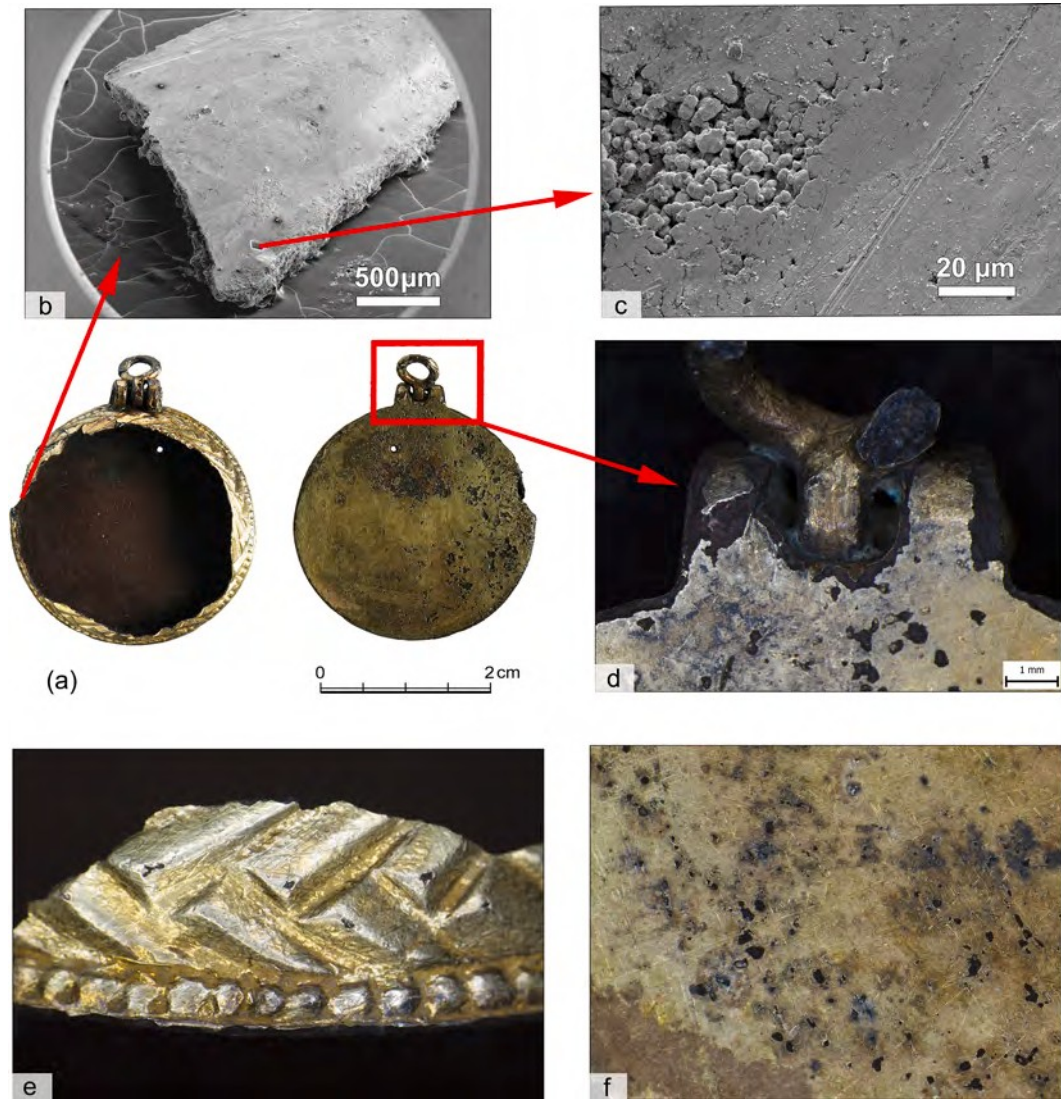


Fig. 3. Medallion H52-2: a - front and reverse views; b-c - detail of the studied fragment showing area next to burnished surface, a porous unburnished area with granular gold - SEM micrographs (SE); d - detail of the suspension system; e - detail of the chased gilded bezel; f - pitting of the gilding layer.

the core and gilding layer. However, as the sample is tilted 52°, vertical measurements of observed structures have to be corrected and EDS analyses can only be semi-quantitative.

(ii) The second approach is the slicing of the materials from the previous cross-section (Li et al., 2018), allowing more accurate analysis and a more complete observation. It involves extracting a lamella with a thickness of about 2 μm and laying it flat on a support (0° tilt). This preparation is very similar to that used for preparing lamella for transmission electron microscopy. It can also be used for extended applications such as determining the crystalline structure of phases and quantitative microstructural analysis by electron backscattered diffraction analysis (EBSD) (Northover and Northover, 2012). The detailed method is shown in Fig. 5. After cross-sections are taken on both sides of the platinum deposit (Fig. 5a–b) according to the aforementioned procedure (i), the specimen is then partially cut out (Fig. 5c) and a W needle is fixed applying platinum on one edge (Fig. 5d–f). In the SEM chamber, the sample is then lifted out *in situ* (Fig. 5g–h), carefully transferred (Fig. 5h–i) and attached to a molybdenum support grid (Fig. 5j–k). The thinning of the specimen can then proceed using a gradual cross-section cleaning milling pattern, with a final milling beam current of 0.79 nA (Fig. 5l). The Mo support with the lamella is then laid flat (0° tilt) on the microscope holder. The complete preparation time is about three hours

to get a 50 μm wide, 30 μm deep and 2 μm thick slide.

4. Results

4.1. Gilding of the gombik H84-1

Fig. 6a shows the FIB cross section of the gilded fragment reported in Fig. 1 and Fig. 4. The gilding was partially covered with cuprous oxide according to EDS analysis.

The FIB cross-section revealed a thick gilding layer ranging from 6 to 9 μm on the copper substrate, which is mainly oxidised in cuprous oxide. Some wide porosities and grain boundaries due to burnishing are observed (Fig. 6a). In addition, smaller voids less than a few hundreds of nm wide are evidenced just above the internal gold layer/copper bulk interface (Fig. 6c).

As revealed by the electronic channeling contrast observed at low beam energy (5 kV) in Fig. 6a and c and by grain size diameter and boundary map from EBSD in Fig. 6d, the gilding is composed of two sub-layers with a different metallurgical morphology:

- (i) a thick gold one on the top part with equiaxed grains of a few μm (green and orange in Fig. 6d), thermic twins here corresponding

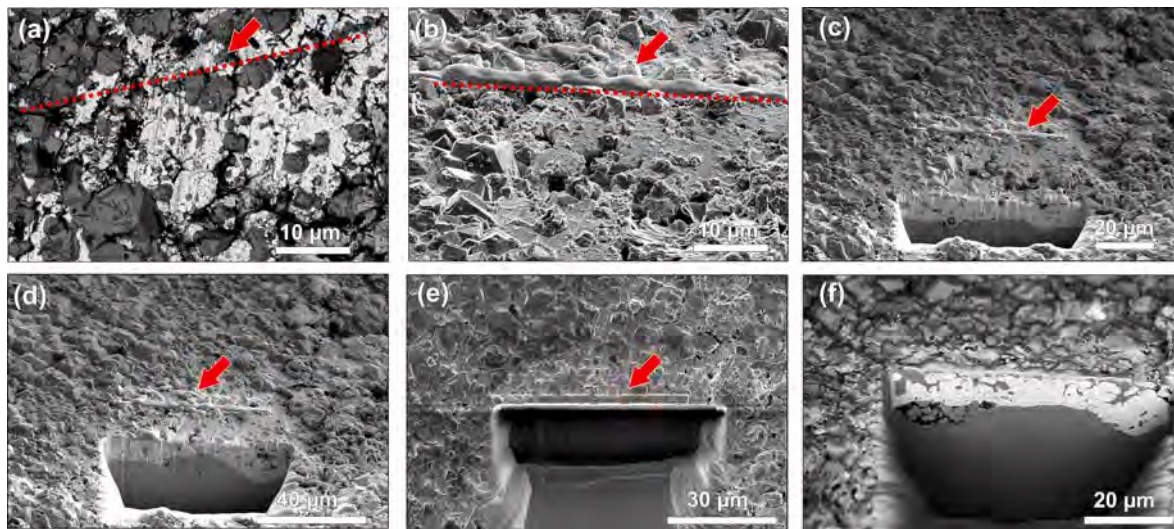


Fig. 4. *In situ* FIB cross-section preparation on the fragment of gilded *gombik* H84-1 (SE and BSE images): **a** - surface observation (BSE mode) and selection line for cross-section; **b** - Pt layer deposit (red arrow) protecting the selected surface before FIB milling (52° tilted); **c-d** - milling operation up to protective Pt layer (red arrow) using a focused beam of Ga⁺ ions; **e-f** - cross-section pit obtained after milling: observation tilted at 0°(e-) and 52°(f-).

To $\Sigma 3$ twin boundaries (misorientation of 60° around $\langle 111 \rangle$) and no evidence of crystal preferential orientation, data that are very characteristic of an annealed structure;

- (ii) a submicrometric Cu-rich sublayer at the interface with the copper substrate (840 nm in Fig. 6c), with nanometric grains (between 50 nm up to a few hundred nm, in blue in Fig. 6d) and incorporating the thin voids mentioned above.

This two-layer structure is also evidenced from X-ray mapping as shown in Fig. 6b. EDS elemental analysis of the gilding revealed a quaternary Au (Hg, Ag, Cu) alloy, the chemical composition of which is not uniform and varies with depth. In addition, according to the X-ray mapping and X-ray line quantitative profiles reported in Fig. 6b and Fig. 7a, respectively, this structure is directly related to a difference of composition:

(i) In the gold top sublayer, the Au content is 70–81 wt%, Hg varies between 10 and 18 wt%, while the Ag maximum is about 4 wt% in the centre of the gold sublayer. The copper value on top of the gold sublayer is around 2 wt%, but due to diffusion, its content is much higher in its internal part;

(ii) the Cu-rich inner sub-layer corresponds to an interdiffusion of Cu and Au elements, as revealed by a marked decrease of Hg and the absence of Ag.

The X-ray profiles of elements Au, Hg, and Cu (Fig. 7a) confirm the presence of an interdiffusion zone at the gilding/copper bulk interface. The diffusion of copper within the gilding layer is clearly evidenced. The mercury is higher in the middle of the gilding thickness and appears to diffuse into the copper substrate like to gold. A plateau of composition is evidenced in the inner sublayer (arrow located at 9 μm in Fig. 7a), with Au ~ 66–68, Hg ~ 9–10 and Cu ~ 23–25 wt%, corresponding to atomic ratios Au/Cu ~ 1 and Au/Hg ~ 7. This point is discussed below.

Furthermore, alteration of the copper substrate is observed under the gilded layer forming cuprous oxide (Fig. 7a). In addition, cuprous oxide is also present in some porosities within the gilding layer. However, it is difficult to determine whether this is due to heating during the initial soldering or gilding processes, or to corrosion in the archaeological soil.

4.2. Gilding of the *gombik* H115-9

The optical observation of the pair H115-8/-9 (Fig. 2) revealed high-quality jewels with a relatively homogeneous gilding surface. The selected area for making the FIB cross-section on the fragment of *gombik*

H115-9 is representative of this aspect. Observation of the sliced cross-section (Fig. 8a) showed a thin gold layer $2 \pm 0.5 \mu\text{m}$ thick, homogeneous and compact without wide porosities and grain boundaries due to burnishing.

As evidenced from the electron channeling contrast image (Fig. 8a–c), the metallographic structure is also a two-sublayer one with characteristics similar to the previous gilding:

- (i) a thick gold sub-layer with an annealed structure, with annealed twins and equiaxed grains, also revealing some curved grain boundaries relative to grain growth during heating;
- (ii) an inner one with nanometric grains, here very thin, ranging from 50 to 300 nm.

The global composition of the gold top sublayer from EDS analysis of the sliced cross-section is in wt%: Au 76, Hg 17, Cu 5 and Ag 2. The interdiffusion sublayer, clearly observed previously on *gombik* H84-1, is not highlighted here, the inner sublayer being very thin and at the limit of the spatial-resolution of the X-ray analysis.

Under the gilding, the copper base substrate was a bronze probably with a low tin content. As shown in Fig. 7b and 8a–c, it is deeply oxidised revealing copper oxide (in grey) surrounded by decuprified areas enriched in tin content (in bright grey), with a Cu/Sn weight ratio ranging from 2 to 4.

It should be noted that for sample H115-9 (gilding on low-tin bronze), no Sn element from the bulk material was found in the gilding, indicating that unlike copper, the tin alloying element did not diffuse into the gilding when heated.

4.3. Gilding of medallion H52-2

As shown in Figs. 3 and 5, the surface of the gilded fragment is clean but the burnishing grooves and porous surface with typical granular structure (globules) in recesses are still well observable. As shown in Fig. 9, the FIB cross-section integrates both burnished and granular Au (Hg) gilding. The thickness of the compact gilded layer is 5.8–7.6 μm (Fig. 9a, d), including porosities between the flattened gold-mercury grains due to insufficiently effective burnishing. Thanks to electron channeling contrast (Fig. 9b, d), a two-sublayer gilding with an annealed metallurgical structure is evidenced on the Cu-base substrate. It is also marked by a thick top gold sublayer and a submicrometric (~350 nm) inner one richer in Cu.

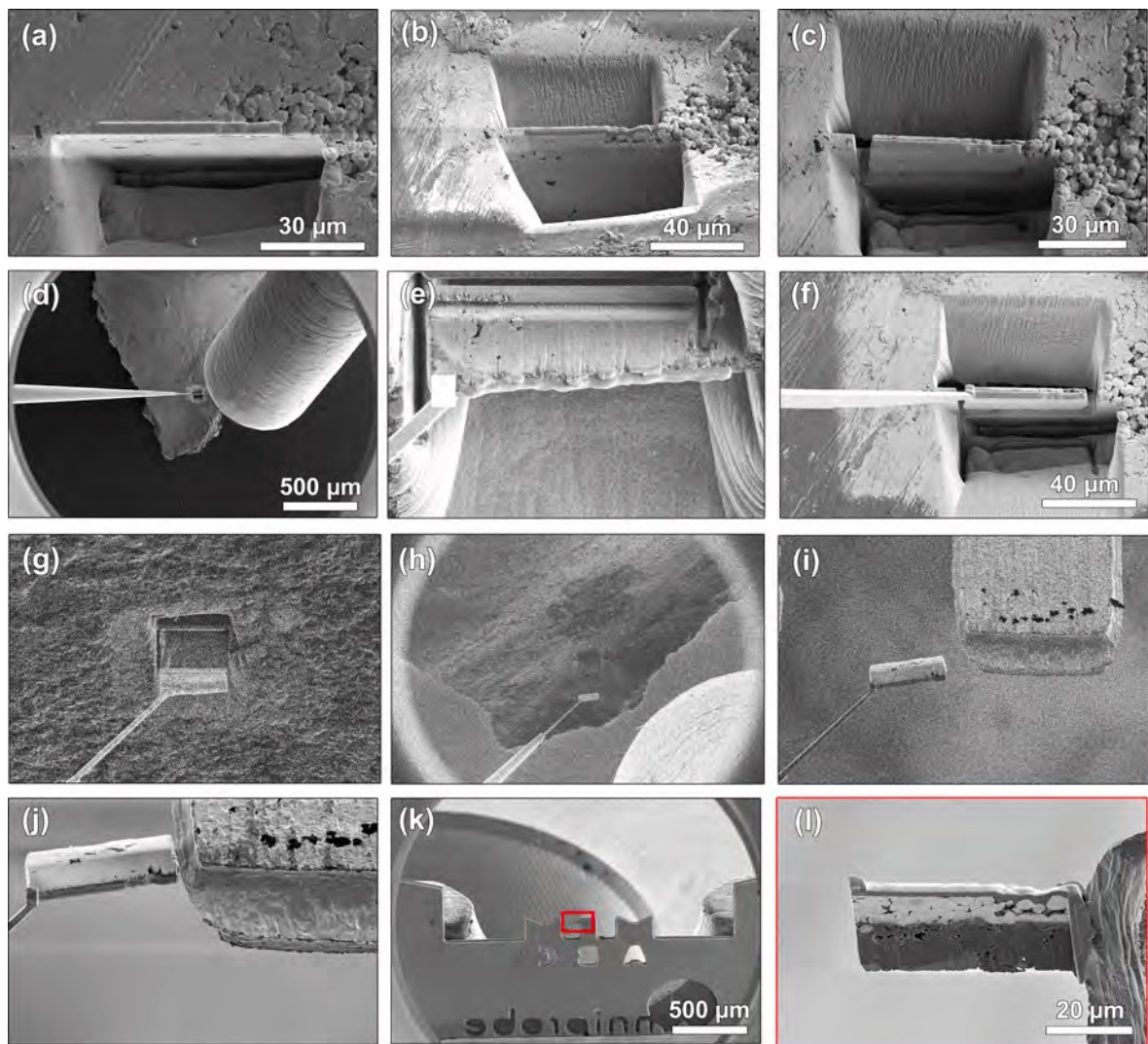


Fig. 5. FIB lift-out technique: Secondary electron and ion SEM images showing the different stages of producing an *in-situ* lamella of the gilded fragment from medallion H52-2: a - cross-section obtained after milling the sample using focused beam of Ga ion (SEI); **b** - abrasion on both sides of the platinum coating; **c** - separation of the lamella from the bulk with a U-shaped milling pattern; **d** - insertion of the micromanipulator and GIS Pt into the chamber; **e-f** - attaching the micromanipulator tip; **g-h** - lifting-out of the lamella; **i-j** - lamella transfer to Mo grid with micromanipulator; **k-l** - wide and detailed view of the fixed lamella on the Mo grid.

The gold sublayer is a quaternary Au-Hg-Ag-Cu alloy. Its global composition in wt.% is: Au ~ 76.5, Hg ~ 17.5, Ag ~ 3.5 and Cu ~ 2.5. The copper content varies markedly with the depth distribution as shown in the X-ray profile of Fig. 7c. For mercury (Hg), its content is lower in the top surface and at the interface with the substrate. The inner sublayer is relative to the heterodiffusion of Au and Cu at the interface gilding/Cu base substrate, probably making a specific metallic phase as indicated by the arrow in Fig. 7c.

In the gold sublayer as shown in Fig. 9d, Au (Hg, Ag, Cu) globules are observed and a sintering effect due to heating is revealed. Within these globules that form grains of a few μm in length, an annealed structure is seen. The impact of sintering on the composition of Au (Hg, Ag, Cu) globules, not in contact with the substrate, is reported in Fig. 9e with the X-ray line profiles of the main elements. A decreasing gradient of the mercury content is revealed from the centre to the external part of the globules, from ~ 21 wt% in the middle of the globule to ~ 15 wt% on the edge. This is directly related to its evaporation during heating. Conversely, the minor Ag and Cu elements do not show significant variation into the Au (Hg, Ag, Cu) metallic phase.

Underneath the gilding layer, the copper base substrate contained a small amount of silver (Ag ~ 1.5–2 wt%) as well as traces of Sn and Fe.

However, the copper substrate is corroded, forming cuprous oxide, with small amounts of Cl (<1 wt%), and has large porosities due to copper dissolution, in which precipitates of silver particles can be observed (in white in Fig. 9d).

5. Discussion

The results obtained in the present work invite certain considerations, including the quality of gilding according to skill level and the identification of the metallurgical structure and phases of the gilding.

5.1. Skill level, quality of the finds versus workshops and origins

In addition to the size of the artefact and the decoration type, which are the basic parameters of comparison, the technical consideration enables the identification of fine products produced by highly skilled and knowledgeable jewellers operating in a courtly environment, and coarse imitations produced by local and less experienced craftsmen (Ottenwelter et al., 2020; Ottenwelter, in press). This technical consideration is mainly linked to the mounting concept, the choice of material (base material, gilding layer, type of solder), the quality of the

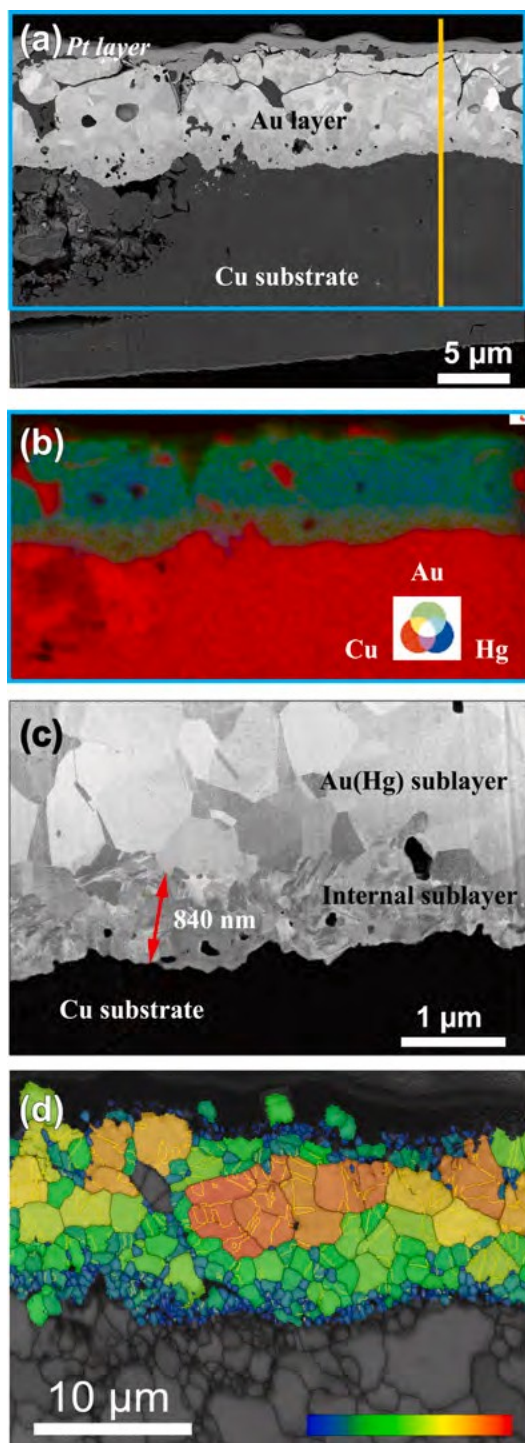


Fig. 6. Gilding of gombik H84-1: a - general view of the gilding layer (BEI - Tilted 0°) – yellow line = X-ray profile of Fig. 7a; b - RGB false colour image (SEM-EDS X-ray maps) of Cu (red), Au (green) and Hg (blue) from the area denoted by a rectangle in b, revealing on the copper substrate (in red) the two-layer structure of the gilding: in green-blue, top Au-Hg sublayer with red Cu oxide inclusions and in green-yellow, thin Cu-rich inner sublayer corresponding to small grains observed in c; c - microstructure of the sliced gilding layer revealing a two-layer structure, with very thin grains at the gilding/copper substrate interface (BEI - Tilted 0°); d - grain size diameter of the layer, ranging from 0 (in blue) to 3 µm (in red) obtained by EBSD. High angular (misorientation angle over 10°) and annealing twin boundaries are indicated in black and yellow, respectively.

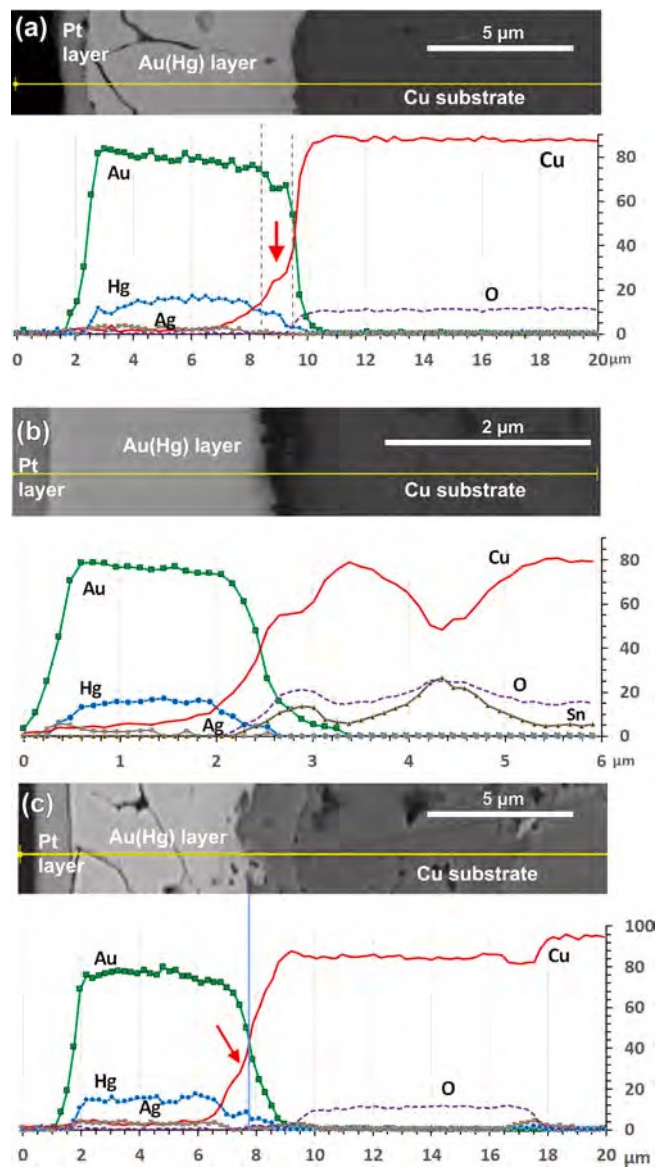


Fig. 7. Cross-sections and X-ray quantitative profiles (normalised wt%) on gilded cross-sections (yellow lines) of: a - gombik H84-1; b - gombik H115-9; c - medallion H52-2. FIB-FEG SEM (20 kV- BEI – Tilt 0°).

mounting, soldering, gilding, tool marks as well as the quality of the decoration. This is particularly important since it can help identifying locally produced artefacts from imported pieces, possibly diplomatic gifts from the powerful neighbouring Christian empires, and can thus demonstrate ties with the Frankish and Byzantine empires (Bülher, 2010; Daim, 2000). The detailed characterisation of the gilding layer enabled access to additional keys of comparison to evaluate the quality of the find.

In this technical context, the first important parameters are the thickness of the gilding layer and its compactness. These two parameters are linked to the quality of the burnishing process; the final step in fire gilding which compacts the porous structure remaining after the evaporation of the mercury, creating a smooth and reflective surface. A dense layer reveals high-quality gilding, while a porous layer indicates poor burnishing and therefore lower gilding skills. Hence, a clear difference in gilding properties and quality is demonstrated between gombik H115-9 and gombik H84-1. As summarised in Table 2, the gilding layer observed on gombik H115-9 is thinner (only 2.1 µm thick in average), very dense and not porous, the opposite of gombik H84-1 and medallion

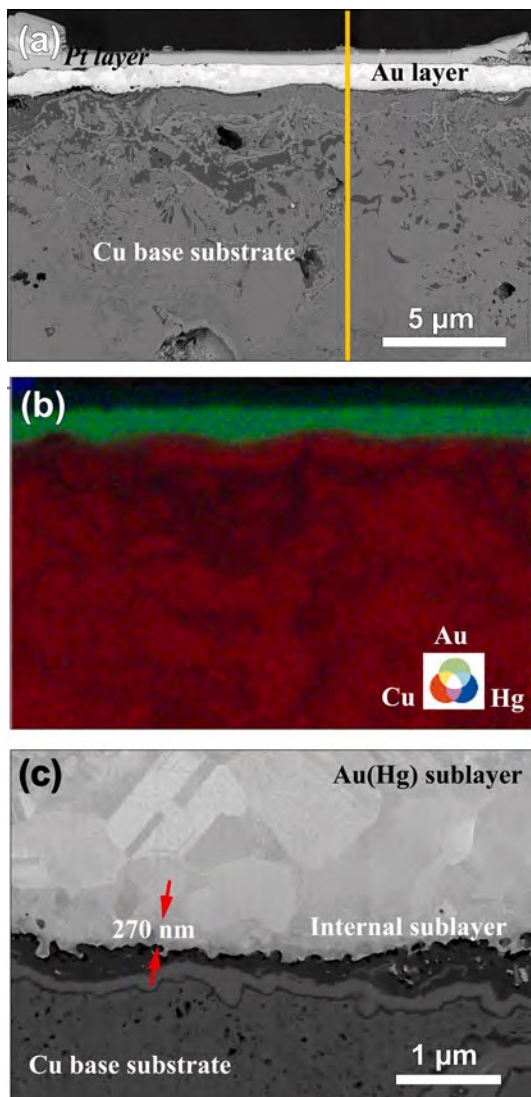


Fig. 8. Gilding of Gombik H115-9: a - cross-section overview (BEI – Tilted 0°) – yellow line = X-ray profile of Fig. 7b; b - Au, Hg and Cu mapping of the milled cross-section a; c - electron channeling contrast of the gilded layer revealing an inner sublayer with nanometric grains on corroded copper base substrate (BE image – 5 kV – Tilted 0°).

H52-2 (around 7.5 µm thick with porosities).

These gilding differences must also be connected to the jewellery quality revealed by the chased decoration. In fact, *gombik* H115-9 was made by a very skilled goldsmith having sketched the motif with a drawing compass. The motifs depicted are very precise and regular in contrast to the motifs of *gombik* H84-1, which were chased less accurately.

As regards the composition of the gilding layer, in all cases quaternary Au-Hg-Cu-Ag gold alloys with similar proportion of Hg, Cu and Ag were produced (Table 2). The composition of the bulk metal showed that different copper base metals were used. Pure copper was used to produce H84-1, but a low tin bronze (Sn ≈ 3–4 wt%) was used for H115-9, while copper with about 1.4 wt% Ag was employed for medallion H52-2. The presence of different metals and impurities reveals the diverse origin of the copper raw materials; recycling was therefore probably the main source of metal used to manufacture these pieces. However, in all the studied cases, the material was sufficient to produce gilded and chased ornament.

The mounting is also a good indication of quality. Both studied *gombiky* have the same construction: a two-hemisphere body

construction and a three-element suspension system (Ottenwelter et al., 2020) soldered with a hard Ag-Cu solder. In both cases, the soldering and mounting is of good quality. The only difference is the pellet present inside *gombik* H84-1 (occasionally present in Bohemian *gombiky*). As regards the medallion, the mounting, especially the one with the suspension system, is reminiscent of Byzantine work (Bosselmann-Ruickbie, 2011, 213–214, 387). Thus, although the quality of gilding is usually related to the quality of mounting and chasing, this does not hold true in the case of this medallion, indicating that good chasing could be related to lower quality gilding, suggesting that the skill level for these two production steps is not always linked.

The iconography depicted in Figs. 1, 2 and 3 on the investigated pieces also reveals cultural origin or influence and could be related to the gilding quality and workshop skills. On the pair of *gombiky* H115-9/8, a rosette in a medallion, a chevron motif and *Manus Dei* are represented. The *Manus Dei* (a clear theocratic symbol), the chevron and rosette motifs have analogies in the Christian and Byzantine world. Similar chevron and rosette motifs can be observed, e.g., on Byzantine chased chalices (Dandridge, 2000, Figs 7.1, 7.5, 7.9).

The motifs on *gombik* H84-1— a peacock with a necklace (Fig. 1f-g) — point to another cultural sphere, i.e., a debased motif of the Sasanian iconography present on fine textiles and silk brocade imported to the Western world via long-distance trade routes from Sogdian, Syria and Iran (Charvát, 1998; Charvát, 2010a, 61; Charvát, 2010b, 20–21). This motif was adopted here, but obviously not understood since the necklace usually represented on Sasanid imagery is represented here as a drop. This could indicate that the motif was chased by a person who did not belong to the same cultural background and therefore that the *gombik* and its gilding were made by a local craftsman.

Hence, the precise characterisation of the gilding layer (thickness, porosity and composition) and of the substrate coupled with the assessment of the quality of the chasing decoration and mounting as well as the iconography investigation reveal that different cultural backgrounds and skills were involved in the manufacture of these pieces of jewellery. It is highly probable that *gombik* H115-9 of high gilding and chasing quality was a diplomatic gift from Byzantium, while *gombik* H84-1 is a local production as confirmed by the quality of its gilding and chased decoration. As regards medallion H52-2, its quality in terms of mounting, chasing, and its uniqueness in the Bohemian context could also indicate a foreign origin.

5.2. Metallurgical characterisation: New results

5.2.1. Fire gilding layer characteristics and structure

Numerous similarities among these mercury gildings have been recorded (Table 2). It has been shown that the gildings have a two-layer structure. This is observed independently of the gilding thickness (from 2 to 10 µm) and of the composition of the copper-base substrate (pure, less pure copper or low-tin bronze). In addition, the gilding layers have an annealing structure characterised by (i) micrometric grains in the upper sublayer 2–10 µm thick and (ii) submicrometric grains in the inner sublayer of hundreds of nm in contact with the copper base substrate.

As regards the (i) thick upper sublayer, all the mercury gildings are quaternary Au-Hg-Ag-Cu gold alloys. Their composition is characterised by a high Hg content (13–18 wt%), with a small amount of Cu and Ag (around 3–4 wt% each). From the X-ray profiles reported in Fig. 7, the elements revealed systematic variations in the gilding: (a) an impoverishment of Hg and Cu contents on the gilding surface, (b) a relative homogeneous composition of Au, Hg, Cu and Ag in the gold sublayer and (c) a pronounced increase of Cu content near the copper base. It is also shown that the variation of composition can result from the sintering of Au (Hg, Ag, Cu) globules, in connection with the vaporisation of mercury and the formation of a gold phase(s) during heating. After burnishing, these globules form flat grains revealing a variation of mercury compositions on a local scale.

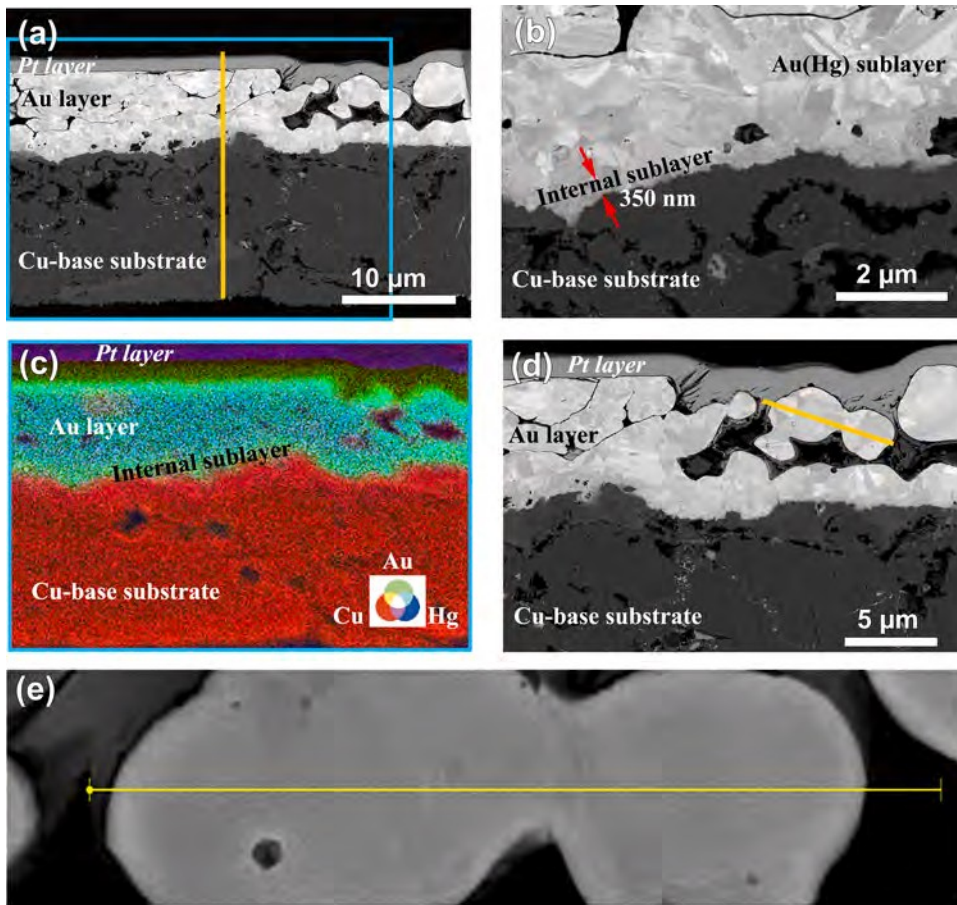
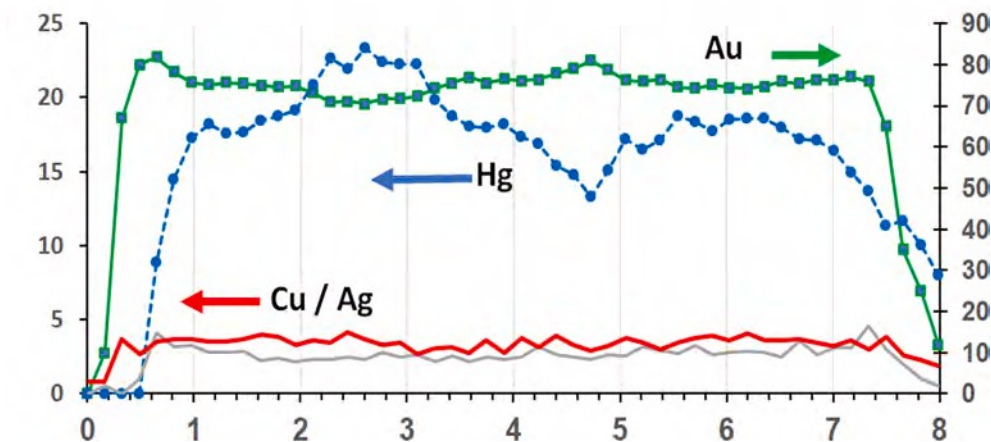


Fig. 9. Medallion H52-2: a - overview of the cross-section (BEI – 5 kV – Tilted 0°) – yellow line = X-ray profile of Fig. 7c; b - grain microstructure revealed by electron channeling contrast showing a very thin inner sublayer (BEI – 6 kV – Tilted 0°); c - corresponding mapping of blue rectangle (in a) showing the repartition of the Au-Cu-Hg elements (in red Cu substrate, in green the Pt protective layer); d - observation of Au (Hg) globules of the layer with sintering evidence; e - X-ray elemental profiles in Au (Hg) globules (yellow line, also in d) (BEI – 20 kV – Tilted 0°).



Concerning the (ii) inner submicrometric layer, the chemical distribution of alloying elements (Fig. 7) revealed a high level of Cu and Au with a very low Hg content and no Ag. The pronounced diffusion profile of Cu is directly related to an interdiffusion phenomenon of copper at the gilding/copper substrate interface. Furthermore, on the X-ray profile of the H84-1 gilding and also for H52-2 to a lesser extent, a composition plateau has been observed (red arrows in Fig. 7a and 7c, respectively).

For H84-1, this plateau can be directly related to the formation of a AuCu (Hg) metallic phase. From the X-ray profiles (Fig. 7a), a composition in wt% close to Au/Cu ~ 1 and Au/Hg ~ 7 was found. A further local EDS analysis of the inner sublayer confirmed this result. Thus, the inner sublayer could be attributed to a stoichiometric AuCu phase, integrating mercury in the AuCu lattice. For H52-2, discontinuity in the

slope of the Cu X-ray diffusion profile in the inner sublayer is also observed for an atomic ratio Au/Cu ~ 1 with a Hg content lower than 10 wt%. For the thinner gilding thickness (H115-9), the Cu diffusion phenomenon is also observed, but the inner sublayer is too thin to allow its characterisation. However, it can be concluded that the small submicrometric grains forming a thin inner sublayer has to be related to one or more AuCu phases additionally comprising mercury.

5.2.2. Fire gilding process: Au-Cu interdiffusion and sintering

It is generally accepted that the fire gilding layer, in comparison to other gilding methods, forms a solid bond, adhering well to the copper base substrate and ideally suited for composite artefacts and those of an irregular shape (Oddy, 1193, Northover and Anheuser, 2000). In this

Table 2

Gilding layer characteristics and estimated main composition at the median position (at a considered length in μm of the gilded layer) determined from X-ray profiles (Fig. 7) and EDS semi-quantitative measurements (20 kV, tilted 0°).

Gilding layer	Parameter of comparison	Gombik H84-1	Gombik H115-9	Medallion H52-2
Au (Hg) gold layer	Thickness (μm)	6–9	1.9–2.5	5–7
	Quality	Uneven	Even	Even with porosities
	Aver. composition wt% (considered length)	Au: 80, Hg: 15; Cu: 2, Ag: 3 (3.75 μm)	Au: 77, Hg: 15.5; Cu:5, Ag: 2.5 (0.8 μm)	Au: 78, Hg: 15; Cu: 3.5, Ag: 3.5 (4.4 μm)
Internal sublayer	Thickness (nm)	400–750	100–250	200–500
	Main composition wt% at the median position	Au:70, Cu:22, Hg:8 (Ag < 0.5)	ND	ND
Substrate	Metal type	Pure copper	Low-tin bronze	Copper (Ag)
		Oxidation (cuprous oxide)	Important oxidation (decuprification)	(Ag ~ 1.4 wt%)
	Condition			Important oxidation

ND: not determined (too thin for allowing resolved EDS analysis).

case, FIB milling showed that this strong bond is in fact directly linked to these submicrometric AuCu (Hg) grains making a very thin inner sublayer. The formation of a AuCu (Hg) phase(s) has to be related to a combined process involving (i) the interdiffusion of copper and probably gold to a lesser extent throughout the gold/copper base substrate interface, and (ii) the Hg diffusion towards the external sublayer outwards. This double diffusion process is directly proved here from the nanometric voids within this sublayer as shown in Fig. 6c and 9b, d. Known as the Kirkendall effect, these nanopores (diffusion vacancies) are directly related to atomic diffusion of the chemical elements occurring at different diffusion rates during the thermal annealing.

In addition to inducing an interdiffusion bonding, the heating process plays a major role in the growth of the micrometric gold grains in the upper sublayer. Heating not only allows the evaporation of mercury but also favours the sintering process of gold globules in the gilding layer, as shown in Fig. 9e for gold grains without contact with the copper substrate. It is revealed that this sintering process is accompanied by the diffusion of mercury from the centre of the grains and its selective release from their surface. In contrast, for Ag and Cu, already present in the initial gold amalgam alloy, their content remains constant in the metal grains and no particular diffusion behaviour seems to occur.

5.2.3. Phase identification and temperature applied

The fire gilding process involves heating an amalgam, initially a paste with a solid gold phase(s) and liquid metallic mercury. After heating the artefact, residual mercury is always encountered in the gilding, with a content of 8–25 wt%, which is confirmed in this case. As demonstrated by Northover and Anheuser (2000, 118–119), the residual Hg content correlates to the temperature applied. At a temperature of 200–250 °C, the evaporation process of the metallic mercury rapidly occurs after a few minutes and the silver-coloured Au₂Hg forms. At this stage, a yellow solid Au₃Hg phase can develop with the release of mercury. This phase is also defined as the ζ phase with a close hexagonal-packed (chp) structure (Okamoto and Massalski, 1989). According to the experimental work of Northover and Anheuser (2000), the final temperature range for fire gilding could be 250–350 °C, below the boiling point of mercury (357 °C), without exceeding a heating time of 15 min.

However, in this study, channeling electron emission and EBSD revealed a gilding layer exhibiting a typical annealing structure for both sublayers (Figs. 6, 7, 8 and 9), indicating the probable formation of fcc phases. The only crystal structure reported from Au-Hg and Au-Cu binary phase diagrams (Okamoto and Massalski, 1989, Fedorov and Volkov, 2016) which fits the electron diffraction signal is the cubic Au-Cu solid solution (space group Fm-3 m). Note that the orthorhombic AuCu P4/mmm phase structure cannot be excluded, despite a less satisfying solution (mean angular deviation of 0.97° instead of 0.52° for Fm-3 m). Neither the hexagonal or orthorhombic symmetry matches, disculping respectively an $\alpha 1$ or Imma AuCu structure.

Even if reliable data on all ternary and quaternary Au-Hg-Ag-Cu

systems is not available yet (Chudnenko and Palyanova, 2016), it can be assumed that the heating process occurred at a temperature above or higher than 380 °C, according to assessed binary and ternary phase diagrams (Okamoto and Massalski, 1989; Chudnenko and Palyanova, 2016; Fedorov and Volkov, 2016). In fact, the fcc metallic phases can only be formed at this temperature or higher, while the other metallic phases mentioned in the literature such as Au₃Hg (ζ) and Au-Hg $\alpha 1$ phases or AuCu₃ (I or II) have a close hexagonal close-packed structure. Thus, according to the composition measurements, both the fcc gold terminal substitutional solid solution Au (Hg, Ag, Cu) for the upper thick gold sublayer and a fcc AuCu(Hg) phase in the inner submicrometric sublayer could be reasonably assumed.

Therefore, from this identification of the crystalline phases of these medieval gildings, the temperature applied during fire heating can be estimated at around 400 °C, a value in good agreement with the highly oxidised substrate observed at the gilding interface, as reported by Northover et al., (2000, 114–120). However, this value is higher than the boiling point of mercury (357 °C) and higher than expected from experimental archaeology. Greater certainty on the crystalline structures of the gilding layers is still needed. This could be achieved by a complementary quantitative structural investigation, such as those performed from EBSD and TEM (transmission electron microscopy) experiments.

6. Conclusion

FIB FEG-SEM is a remarkable tool for examining thin, fragile and complex surface structures of cultural heritage materials such as gilded metals (up to 20 μm deep). It allows simplification of sample preparation, which is much easier and faster and avoids stress and surface modification, as no resin embedding or surface polishing are performed. It is a very interesting method for local investigation of ancient materials, as it can be considered as a rather non-invasive method. This method is promising for larger applications on a wide range of ancient and historical materials – biological, organic and mineral.

This study of the fire-gilded layer on elite jewellery reveals that the gilding is characterised by a two-sublayer structure, the external being a quaternary Au-Hg-Cu-Ag alloy attributed to the terminal fcc Au solid solution, and an inner sublayer formed by submicrometric metallic grains of an AuCu intermetallic phase that has not been precisely determined.

The identification of (fcc) crystalline phases and the presence of a highly oxidised substrate at the gilding/copper base substrate interface indicate that the heating temperature was probably around 400 °C. Furthermore, it was shown that heating the gilding layer not only allows the evaporation of mercury but also promotes a sintering process between the gold grains.

The precise characterisation of the gilding layers provided useful elements to identify different levels of skills in fire gilding and the overall quality of the finds. Hence, it was shown that a thin and dense

layer of gilding indicated high gilding skill, while a thick and porous layer suggested a lower skill level.

Declaration of Competing Interest

The authors declare that they have no known competing financial interests or personal relationships that could have appeared to influence the work reported in this paper.

Acknowledgments

We are extremely grateful to Dr. J. Frolík for the opportunity to work on these extraordinary pieces of jewellery.

Funding

This research was supported by institutional supports (RVO: 67985912 – the Czech Academy of Sciences, Institute of Archaeology, Prague, and the CNRS, UMR 5608, research group METAL).

Data availability

The raw/processed data required to reproduce these findings cannot be shared at this time as the data also forms part of an ongoing study.

References

Anheuser, K., 1997. The Practise and Characterization of Historic Fire Gilding Techniques. *JOM (J. Miner., Met. Mater. Soc.)* 49, 11, 58–62.

Bühler, B., 2010: Is it Byzantine metalwork or not? Evidence for Byzantine craftsmanship outside the Byzantine Empire (6th to 9th centuries AD) In: Daim, F. & Drauschke, J. (Eds.) *Byzanz - Das Römerreich im Mittelalter. Teil 1. Welt der Ideen, Welt der Dinge*, Mainz 2010, 84, 1, 213–234.

Benda, K., 2002. *Ornament and Jewellery. Archaeological Finds from Eastern Europe, Svoboda, Prague.*

Bosselmann-Ruickbie, A., 2011: Byzantinischer Schmuck des 9. bis frühen 13. Jahrhunderts, Untersuchungen zum metallenen dekorativen Körperschmuck der mittelbyzantinischen Zeit anhand datierter Funde. Reichert Verlag Wiesbaden, Reihe B: Studien und Perspektiven, Band 28.

Charvát, P., 1998. *Dálkový obchod v raně středověké Evropě (7.–10. století)*. Masaryk University, Faculty of Arts, Brno.

Charvát, P., 2010a: The Emergence of the Bohemian state. *East Central and Eastern Europe in the Middle Ages, 450–1450*, vol. 13, Brill: Leiden – Boston.

Charvát, P., 2010b: 2010b: Slyšte volání muezzinovo – České země a arabský svět ve starším středověku (do roku 1300). *University of West Bohemia in Plzeň Plzeň*

Chiavari, C., Bernardi, E., Balbo, A., Monticelli, C., Raffo, S., et al., 2015. Atmospheric corrosion of fire-gilded bronze: corrosion and corrosion protection during accelerated ageing tests. *Corros. Sci.* 100, 435–447.

Chudnenko, K.V., Palyanova, G.A., 2016. Thermodynamic modeling of native formation of Au–Ag–Cu–Hg solid solutions. *Appl. Geochem.* 66, 88–100.

Daim, F. (Ed.) 2000: *Die Awaren am Rand der byzantinischen Welt. Studien zu Diplomatie, Handel und Technologietransfer im Frühmittelalter (The Avars on the border of the Byzantine world, diplomacy, Trade and the transfer of Technology in the Early Middle Ages)* Innsbruck 2000.

Dandridge, P., 2000. A study of the Gilding of Silver in Byzantium In: *Gilded Metals: History, Technology and Conservation* / ed. by Terry Drayman-Weisser; Archetype Publication, American Institute for Conservation of Historic and Artistic Works (AIC), 123–143.

Fedorov, P.N., Volkov, S.N., 2016. Au-Cu phase diagram. *Russ. J. Inorg. Chem.* 61, 772–775.

Frolík, J., 2014: Pohřebiště v Lumbeho zahradě, Analýza, chronologie, význam. In: J. Frolík et al., *Pohřebiště v Lumbeho zahradě na Pražském Hradě, Díl II. Studie, Castrum Pragense 12, Prague, 5–116.*

Frolík, J., Smetánka, Z., 2014: Pohřebiště v Lumbeho zahradě na Pražském Hradě, Díl I. *Katalog. Castrum Pragense 12, Prague.*

Goldstein, J.I., Newbury, D.E., Echlin, P., Joy, D.C., Lyman, C.E., et al., 2003. *Scanning Electron Microscopy and X-ray Microanalysis*, 3rd ed. Springer, New York.

Gunter, A.C., Jett, P., 1992. *Ancient Iranian metalwork in the Arthur M. Sackler Gallery and the Freer Gallery of Art, Arthur M. Sackler Gallery and Freer Gallery of Art, Washington.*

Johnson, D., Kearns, S., Grady, M.M., 2012. Subsurface analysis by application of FIB-SEM to sample of geological and historical importance. In: *Historical technology, Materials and Conservation, SEM and Microanalysis*, eds. N. Meeks, C. Cartwright, A. Meek, A. Mongiatti: 2012, Archetype publications, London, 56–68.

Jett, P., Chase, W.T., 2000: *The gilding of Metals in China* In: *Gilded Metals: History, Technology and Conservation* / ed. by Terry Drayman-Weisser; Archetype Publication, American Institute for Conservation of Historic and Artistic Works (AIC), 145–155.

Li, C., Habler, G., Baldwin, L.C., Abart, R., 2018. An improved FIB sample preparation technique for site-specific plan-view specimens: A new cutting geometry. *Ultramicroscopy* 184, 310–317.

Masi, G., Chiavari, C., Avila, J., Esvan, J., Raffo, S., et al., 2016. Corrosion investigation of fire-gilded bronze involving high surface resolution spectroscopic imaging. *Appl. Surf. Sci.* 2016, 317–327. <https://doi.org/10.1016/j.apsusc.2016.01.101>.

Masi, G., Esvan, J., Josse, C., Chiavari, C., Bernardi, E., et al., 2017. Characterization of typical patinas simulating bronze corrosion in outdoor conditions. *Mater. Chem. Phys.* 200, 308–321.

Murakami, R., 2000: *Archaeological Gilded Metals Excavated in Japan*, In: *Gilded Metals: History, Technology and Conservation*, ed. Terry Drayman-Weisser; Archetype Publication, American Institute for Conservation of Historic and Artistic Works (AIC), 157–168.

Northover, P., Anheuser, K., 2000. *Gilding in Britain: Celtic, Roman and Saxon*. In: *Drayman-Weisser, T. (Ed.), Gilded Metals, History, Technology and Conservation*. Archetype Publication, pp. 109–121.

Northover, S.M., Northover, J.P., Meeks, N., Cartwright, C., Caroline, Meek, A., Mongiatti, A., 2012. *Applications of Electron Backscatter Diffraction (EBSD) in Archaeology*. In: *Historical Technology, Materials and Conservation: SEM and Microanalysis*. Archetype Publications, Cartwright, pp. 76–85.

Oddy, A., 1993. *Gilding of metals in the Old World*. In: Susan La Niece, Craddock, P., (Eds.), *Metal Plating and Patination. Cultural, technical and historical developments*, (171–181).

Oddy, A., 2000. *A History of Gilding with Particular Reference to Statuary*. In: *Drayman-Weisser, T., (Ed.), Gilded Metals, History, Technology and Conservation*. Archetype Publication, 1–19.

Okamoto, H., Massalski, T.B., 1989. *The Au-Hg (gold-mercury) system*. *Bull. Alloy Phase Diagrams* 10, 50.

Otteweller, E., Déd, J., Barčáková, L., 2014. *Technical study of jewellery from the Lumbeho Garden cemetery at Prague Castle*. In: *Castrum Pragense 12, Pohřebiště v Lumbeho Zahradě na Pražském Hradě, Díl II. Studie*, J.Frolík a kolektiv, pp. 163–287.

Otteweller, E., Déd, J., Barčáková, L., 2017. *Early Medieval gombiky from the Lumbeho Garden cemetery, Prague Castle* In: *Materials and Manufacturing processes*, vol.32 (7-8), 836-849.

Otteweller, E., Barčáková L., Josse, C., Robbiola, L., Krupičková Š, et al., 2020. *Technological characterization of early Medieval gilded copper hollow pendants (gombiky), from Mikulčice (Moravia) and Prague Castle (Bohemia)*. *Archaeological and Anthropological Sciences* 12, 145–167. <https://doi.org/10.1007/s12520-020-01084-4>.

Otteweller E. in press: *Early Medieval elite jewellery from Moravia and Bohemia: manufacturing processes, construction, materials, conservation-restoration*. Doctoral thesis, RGZM.

Profantová, N. a kolektiv, 2010. *Klecany. Raně středověká pohřebiště-2. svazek*, Archaeological Institute of the Czech Academy of Arts, Prague.

Profantová, N., 2013. *K změnám ve vývoji hmotné kultury 10. století v Čechách*, In: *Archaeologia historica* / Brno: Masarykova univerzita Roč. 38, no. 1 (2013), pp. 27–44. *Archaeologia historica*, 38/2013/1, Brno.

Sandu, I.C.A., de Sa, M.H., Pereira, M.C., 2011. *Ancient 'gilded' art objects from European cultural heritage: a review on different scales of characterization*. *Surf. Interface Anal.* 43 (8), 1134–1151.

Shin, Y.B., Lee, M.H., Kim, G.H., 2020. *Manufacturing Technique of Gilt-Bronze Objects Excavated from Tomb No.1 (Donghachong) in Neungsan-ri, Buyeo*. *Korean J. Mater. Res.* 30, 453–457.